



# Plasma Flow Generation due to the Nonlinear Alfvén Wave Propagation around a 3D Magnetic Null Point

S. Sabri<sup>1</sup> , H. Ebadi<sup>1</sup> , and S. Poedts<sup>2,3</sup> <sup>1</sup> Department of Theoretical Physics and Astrophysics, Faculty of Physics, University of Tabriz, P.O. Box 51666-16471, Tabriz, Iran; [876.sabri@gmail.com](mailto:876.sabri@gmail.com), [s.sabri@tabrizu.ac.ir](mailto:s.sabri@tabrizu.ac.ir)<sup>2</sup> Center for mathematical Plasma Astrophysics, Department of Mathematics, KU Leuven, Celestijnenlaan 200B, B-3001 Leuven, Belgium<sup>3</sup> Institute of Physics, University of Maria Curie-Skłodowska, ul. Radziszewskiego 10, PL-20-031 Lublin, Poland

Received 2021 July 15; revised 2021 September 1; accepted 2021 September 2; published 2021 November 25

## Abstract

The behavior of current density accumulation around the sharp gradient of magnetic field structure or a 3D magnetic null point and with the presence of finite plasma pressure is investigated. It has to be stated that in this setup, the fan plane locates at the  $xy$  plane and the spine axis aligns along the  $z$ -axis. Current density generation in presence of the plasma pressure that acts as a barrier for developing current density is less well understood. The shock-capturing Godunov-type PLUTO code is used to solve the magnetohydrodynamic set of equations in the context of wave-plasma energy transfer. It is shown that propagation of Alfvén waves in the vicinity of a 3D magnetic null point leads to current density excitations along the spine axis and also around the magnetic null point. Besides, it is pointed out the  $x$  component of current density has oscillatory behavior while the  $y$  and  $z$  components do not show this property. It is plausible that it happens because the fan plane encompasses separating unique topological regions, while the spine axis does not have this characteristic and is just a line without separate topological regions. Besides, current density generation results in plasma flow. It is found that the  $y$  component of the current density defines the  $x$  component of the plasma flow behavior, and the  $x$  component of the current density prescribes the behavior of the  $y$  component of the plasma flow.

*Unified Astronomy Thesaurus concepts:* [Magnetohydrodynamics \(1964\)](#); [The Sun \(1693\)](#); [Alfvén waves \(23\)](#)

## 1. Introduction

In the study of the Sun, magnetic null points that are prevalent in the solar atmosphere play a key role. Due to the magnetic reconnection, null points are considered as places of magnetic energy release and conversion of the magnetic energy into other forms of energy (Parker 1957; Sweet 1958; Priest & Forbes 2000). Since it is nearly impossible to measure the magnetic field of the solar corona, the structure of field lines near the null points defined by coronal loops makes it possible to detect null points. At null points, the strength of the magnetic field (and thus the Alfvén speed) is zero. Three-dimensional X-point structures in the corona were detected in soft X-ray and extreme-ultraviolet ranges (Filippov 1999; Su et al. 2013; Freed et al. 2015).

For every 100 photospheric flux focusings, on average between almost seven and fifteen 3D coronal null points are expected by Longcope et al. (2003) and Close et al. (2004). Local properties of a perturbed 3D magnetic null point has been studied in the linear regime for cold plasma (Rickard & Titov 1996).

Since astrophysical magnetic fields are 3D, to comprehend the plasma heating process, 3D magnetic field structures should be pursued. Galsgaard et al. (2003), Pontin & Galsgaard (2007), Pontin et al. (2007), Galsgaard & Pontin (2011a, 2011b) studied the current density accumulation at the 3D null point, along the spine axis and also at the fan plane without investigation into the behavior of the plasma flow. The behavior of the Alfvén wave near the 3D magnetic null point is investigated by considering the WKB approximation (McLaughlin et al. 2008). It was suggested that the Alfvén wave moved along the magnetic field lines with the equilibrium Alfvén speed and focused along the spine and at the fan plane.

Current density generation at the magnetic null point leads to the Lorentz force that causes the magnetic null-point collapse to drive a current sheet (Pontin & Craig 2005; Craig & Pontin 2014). The excited reconnection may have various forms. The spine–fan reconnection that is most common transfers magnetic flux across the separatrix and releases a significant amount of stored magnetic energy (Pariat et al. 2009; Pontin et al. 2013). There are two other kinds of magnetic reconnection at 3D magnetic null points, torsional–spine and torsional–fan magnetic reconnection that include no flux transfer across the separatrix (Pontin 2011). It is now well understood that 3D magnetic reconnection may also happen in the absence of magnetic null points and separatrices. Due to the structure of the magnetic field, magnetic null points have been proposed as impressive particle acceleration sites around the magnetic nulls (Guo et al. 2010; Stanier et al. 2012). Indeed, when a current sheet is excited at the magnetic null point, because of the associated electric field, the null point can result in particle acceleration. Furthermore, there is observational evidence that reconnection is occurring at the 3D magnetic null point located within the current sheet in the magnetotail of the Earth (Xiao et al. 2006). Hence, studying the properties of the current density generation and its subsequent effect on plasma flow, particularly around the 3D magnetic null points that are also near our planet, could be very important.

Magnetic null-point reconnection has significant importance in realistic 3D structures. It is still an open question what reconnection at null points looks like. In particular, the description of parameters such as current density and plasma flow helps the analysis of the observation. Then in this work, we would like to explore the behavior of current densities and also plasma flow in detail. Attraction of the disturbances to 2D and 3D magnetic null points is studied by Craig & McClymont (1993)

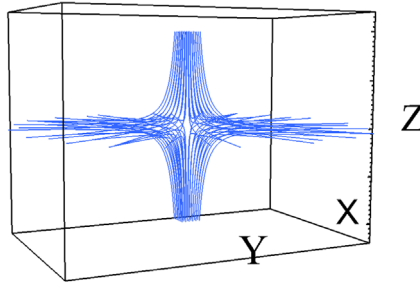


**Figure 1.** Representative field lines with a proper 3D magnetic null point. Three main characteristics of this structure are null point, fan plane, and spine axis that locate at the origin, the  $xy$  plane, and along the  $z$ -axis, respectively.

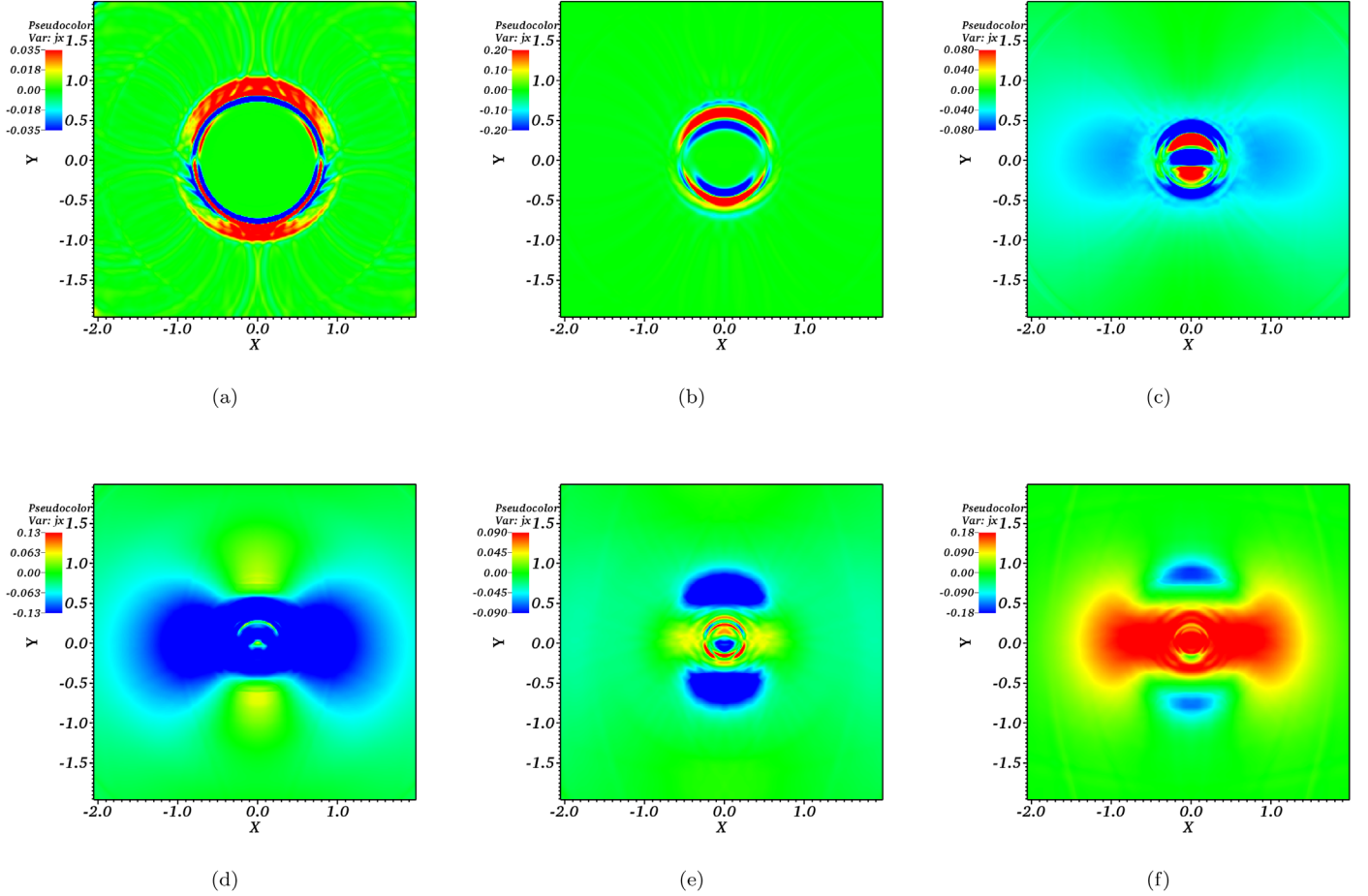


**Figure 2.** Numerical solution of  $j_x$  ( $x$  component of current density) at the fan plane for  $t = 0.3$  s,  $t = 0.5$ ,  $t = 0.7$  s,  $t = 0.9$  s,  $t = 1.0$  s, and  $t = 1.1$  s.

and Galsgaard & Nordlund (1996). Nonetheless, the properties of single 3D magnetic null-point reconnection and its following results are not well known. Then in this study, the properties of current densities and also plasma flow excitation at the complex 3D magnetic null point that are investigated could help the analysis of the observational studies.

The so-called ponderomotive force that is associated with the variation of the magnitude field is the key factor to explain the difference between linear and nonlinear magnetohydrodynamic (MHD) wave behavior (Hollweg 1971; Tikhonchuk et al. 1995). Variation in the absolute value of the magnetic field is accompanied by a steepening of the wave front (Zheng et al. 2016).

A myriad of studies has been done to explore the characteristics of 2.5D X-point topologies (Sabri et al. 2018, 2019, 2020a, 2020b). As a result, Alfvén waves

accumulate along the separatrices without crossing them, whereas fast waves refract around the null point. Therefore, these regions are identified as locations for potential heating by ohmic wave dissipation and implicated as a possible mechanism for localized heating events.

It is theoretically found that the accumulation of disturbances in specific areas can lead to the current sheets excitations. Nevertheless a key question in the solar physic is that how it is possible that at the almost ideal solar corona, huge magnetic reconnection takes place. In real plasma, it is obvious that such high amount of current density excitation in small scales itself causes resistive effects (Pontin & Craig 2005). On the other hand, small scale current density generation conveys magnetic diffusion and reconnection. Thereon, what is less well explored is the

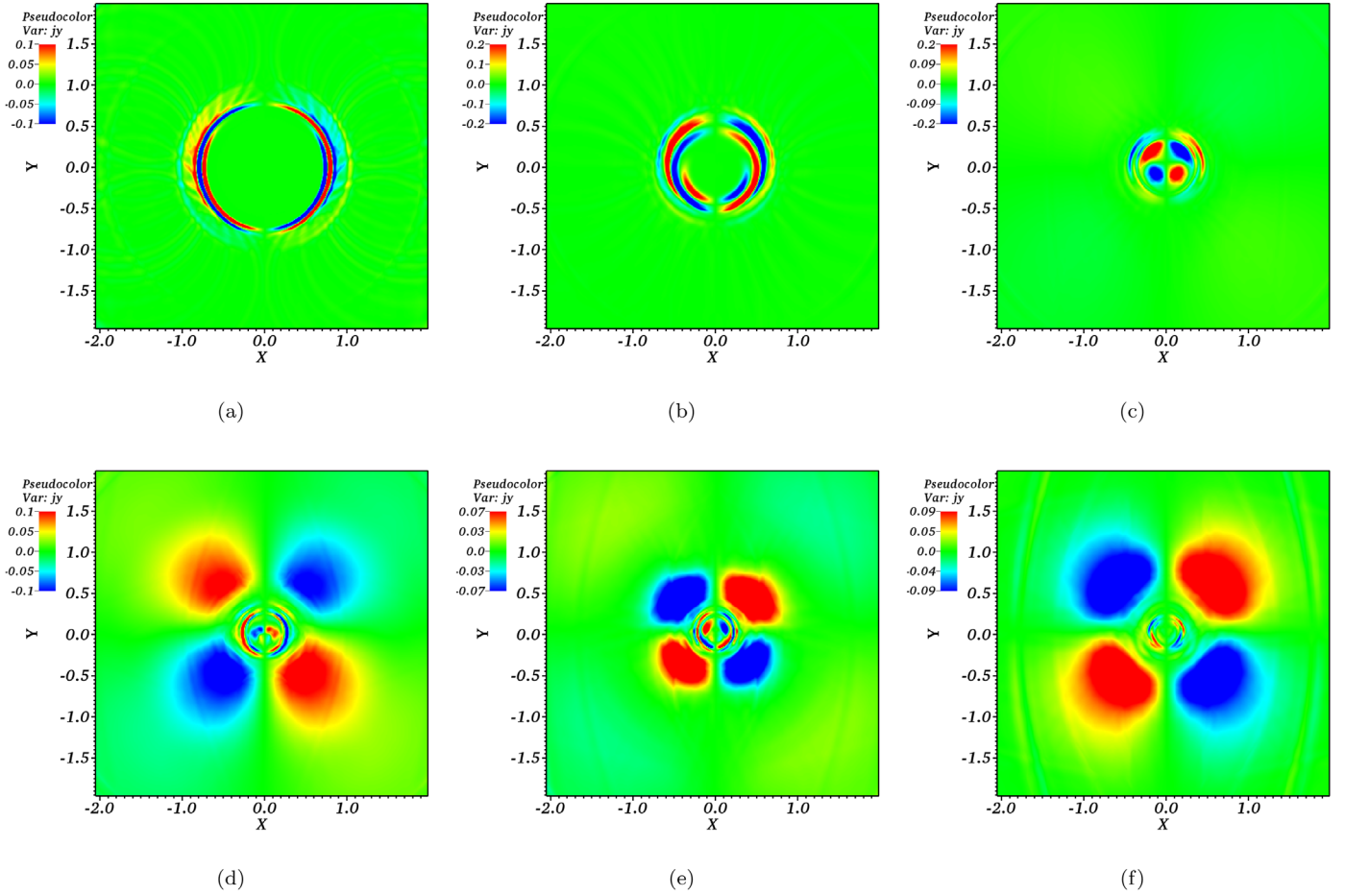


**Figure 3.** Numerical solution of  $j_y$  ( $y$  component of current density) at the fan plane for  $t = 0.03$  s,  $t = 0.5$ ,  $t = 0.7$  s,  $t = 0.9$ ,  $t = 1.0$  s, and  $t = 1.1$  s.

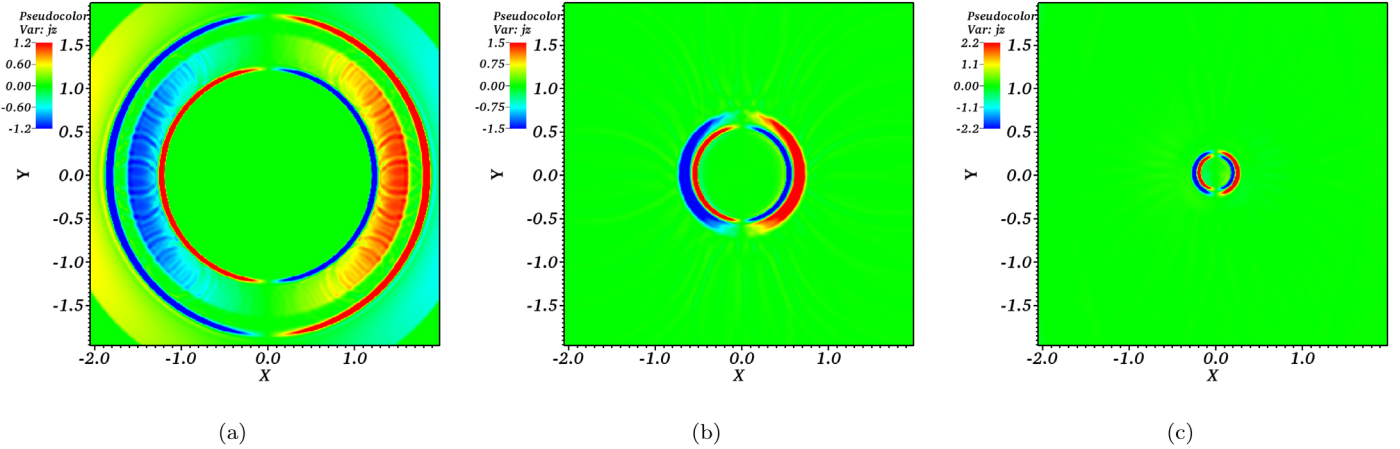


**Figure 4.** Numerical solution of  $j_z$  ( $z$  component of current density) at the fan plane for  $t = 0.1$  s,  $t = 0.5$  s,  $t = 0.6$  s, and  $t = 1.0$  s.

effect of finite plasma pressure on the developing of the current density. Then, we decided to study the current density generation in finite plasma pressure.

In solar physics, Alfvén waves predominantly have a main role in coronal heating because they propagate from lower layers of the atmosphere to the corona (e.g., Ruderman 1999; Srivastava et al. 2017). Copil et al. (2008) suggested that propagating Alfvén waves could locally lead to the coronal plasma heating. However, the efficiency of nonlinear behavior of Alfvén waves around the 3D magnetic null point has not

been given in detail so far. In our previous work (Sabri et al. 2018), we studied dynamics of a similar initial Alfvén wave pulse in the vicinity of a 2.5D magnetic null point. It was shown that a high-amplitude Alfvén wave could be accompanied by nonlinear perturbations of the plasma density. It was found that due to the induced phase mixing, nonlinear Alfvén wave dynamics became more complicated. In the present paper, we consider the same setup and try to find out the effect of the magnetic structure on current density accumulations and their feedback on the plasma flow.

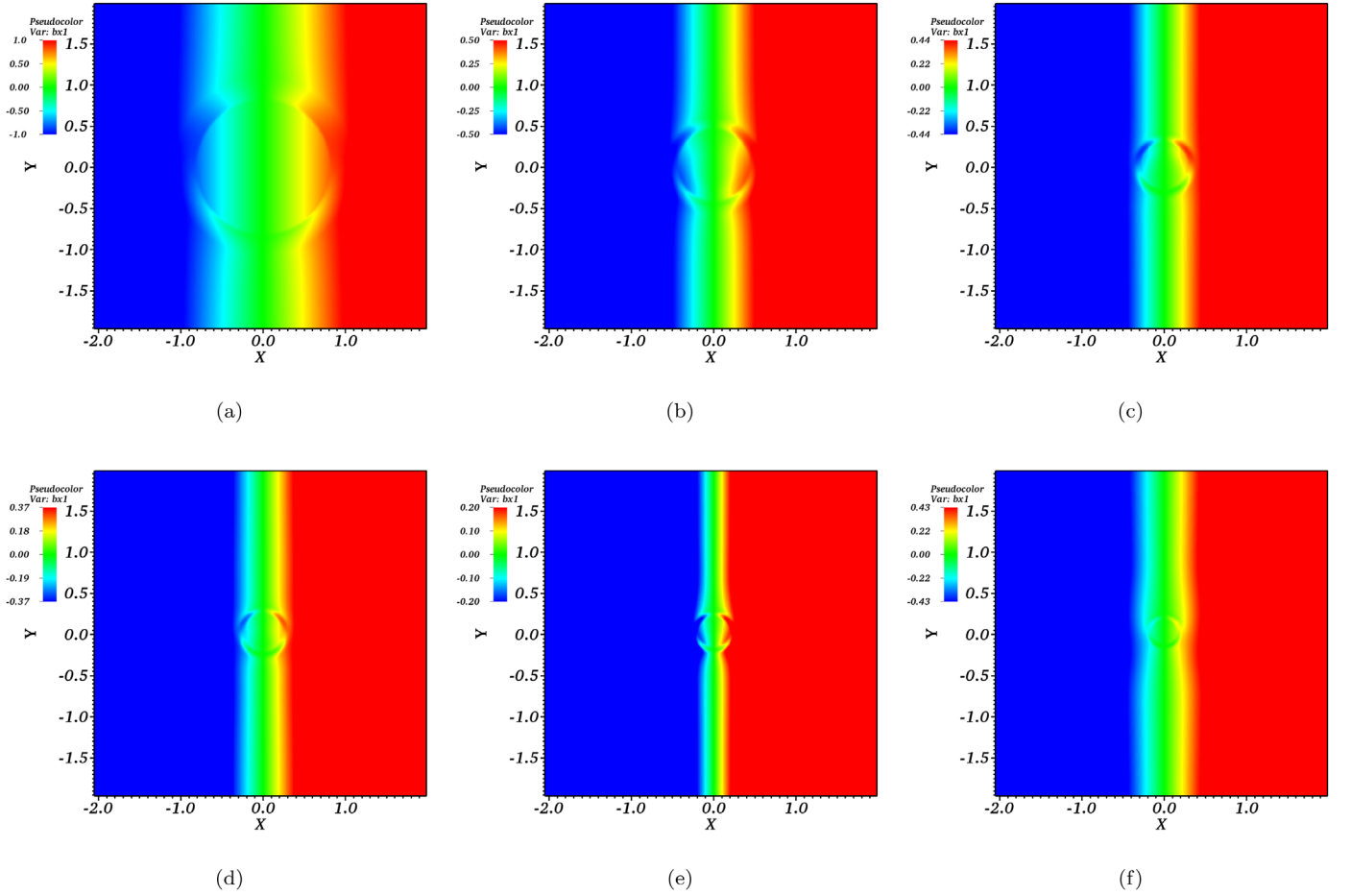


**Figure 5.** Numerical solution of  $b_x$  ( $x$  component of magnetic field) for  $t = 0.0$  s,  $t = 0.6$ ,  $t = 0.8$  s,  $t = 0.9$ ,  $t = 1.0$  s, and  $t = 1.1$  s at the fan plane. It shows the disturbance of the  $x$  component of the magnetic field due to the propagation of the Alfvén wave around a 3D magnetic null point.

The remainder of this paper is organized as follows: In Section 2, we outline the numerical scheme and simulation setup, and in Section 3, we discuss the numerical results and provide a discussion for propagation of Alfvén waves toward the 3D magnetic null point and the evolution of the current density and excited plasma flow. Finally, in Section 4 we provide a brief conclusion and outlook.

## 2. Numerical Scheme and Simulation Setup

The numerical scheme applied in the simulation is described briefly as below. Three-dimensional magnetohydrodynamic equations are solved on staggered meshes, so required MHD preservation laws are automatically satisfied:

$$\rho \left[ \frac{\partial \mathbf{V}}{\partial t} + (\mathbf{V} \cdot \nabla) \mathbf{V} \right] = \left( \frac{1}{\mu} \nabla \times \mathbf{B} \right) \times \mathbf{B} - \nabla P, \quad (1)$$

$$\frac{\partial \mathbf{B}}{\partial t} = \nabla \times (\mathbf{V} \times \mathbf{B}) + \eta \nabla^2 \mathbf{B}, \quad \text{with } \nabla \cdot \mathbf{B} = 0, \quad (2)$$

$$\frac{\partial \rho}{\partial t} + \nabla \cdot (\rho \mathbf{V}) = 0, \quad (3)$$

$$\frac{\partial P}{\partial t} + (\mathbf{V} \cdot \nabla) P = -\gamma P \nabla \cdot \mathbf{V}, \quad (4)$$

where  $\rho$ ,  $\mathbf{V}$ ,  $\mathbf{B}$ , and  $P$  represent, respectively, the mass density, plasma velocity, magnetic field, and plasma pressure. The

constants  $\mu$  and  $\gamma$  denote the magnetic permeability and the ratio of the specific heats, where we have  $\mu = 4\pi \times 10^{-7} \text{ Hm}^{-1}$ ,  $\eta = 10^{-6}$ , and  $\gamma = 5/3$ .

We consider a static ( $\mathbf{V}_0 = \mathbf{0}$ ) background plasma, so there is not any plasma flow from the boundaries. The initial background magnetic field is potential and defines a 3D magnetic null point at the origin:

$$\mathbf{B}_0 = [x, \epsilon y, -(\epsilon + 1)z]. \quad (5)$$

The direction of the predominant field lines is controlled by the eccentricity parameter  $\epsilon$ . The field line structure of this setup is illustrated in Figure 1. For the 3D null point, two important characteristics are the spine line and the fan plane (Priest & Titov 1996). Field lines along the  $z$ -axis that near or relinquish the null point are separated by the spine. The  $z = 0$  plane is recognized as the fan plane that involves radial field lines. Structure of the magnetic field depends on the eccentricity parameter  $\epsilon$  as follows:

- (1) For  $\epsilon = 0$ , there is a simple 2D magnetic null point in the  $xz$  plane.
- (2) For  $\epsilon = 1$ , it is known as a proper magnetic null point that has azimuthal symmetry about the spine axis without any preferred direction of the field lines.
- (3) Magnetic null points with no preferred direction are known as improper nulls.

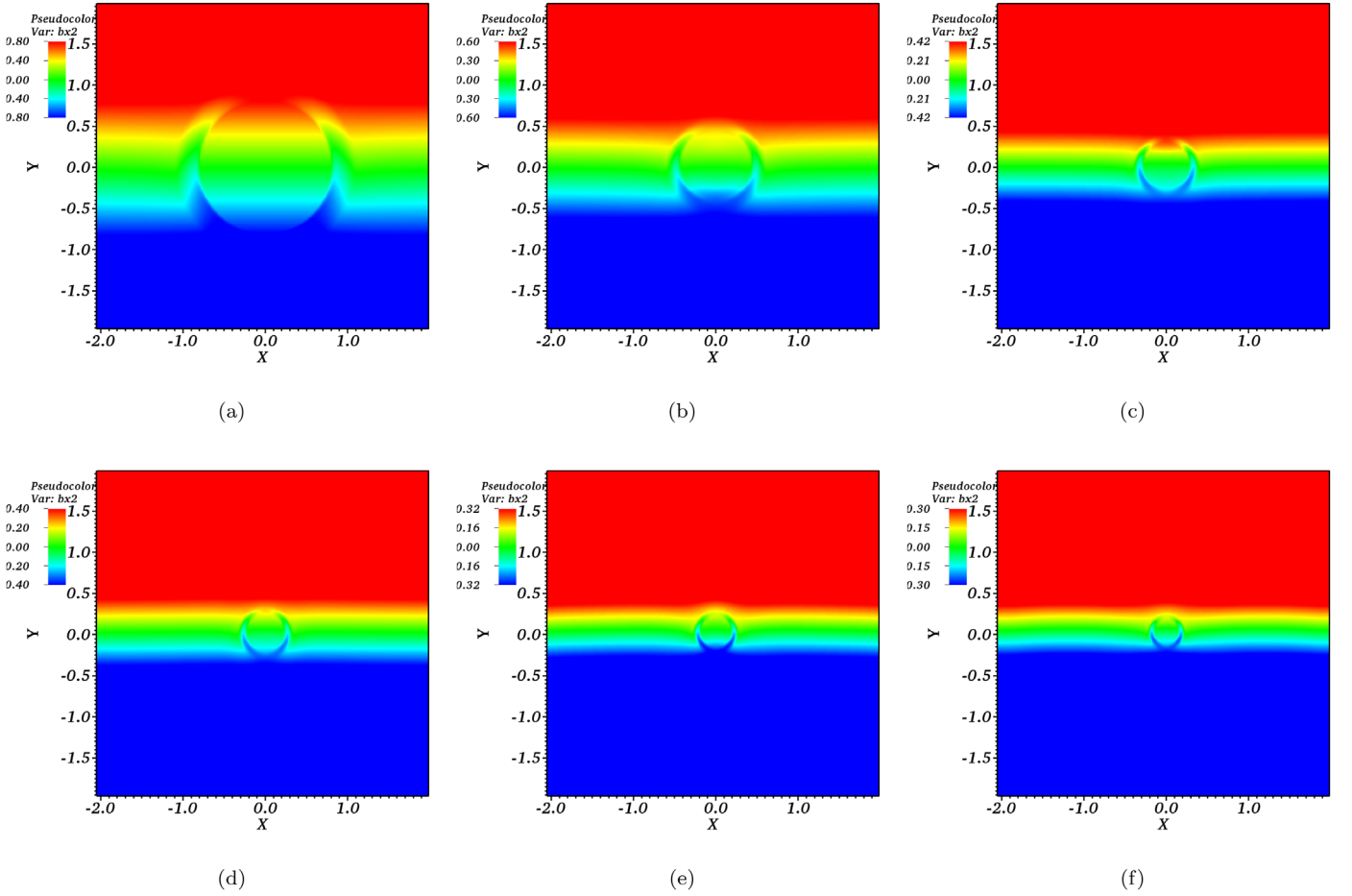


**Figure 6.** Numerical solution of  $b_y$  (y component of magnetic field) at the fan plane for  $t = 0.0.3$  s,  $t = 0.6$ ,  $t = 0.8$  s,  $t = 0.9$ ,  $t = 1.0$  s, and  $t = 1.1$  s.

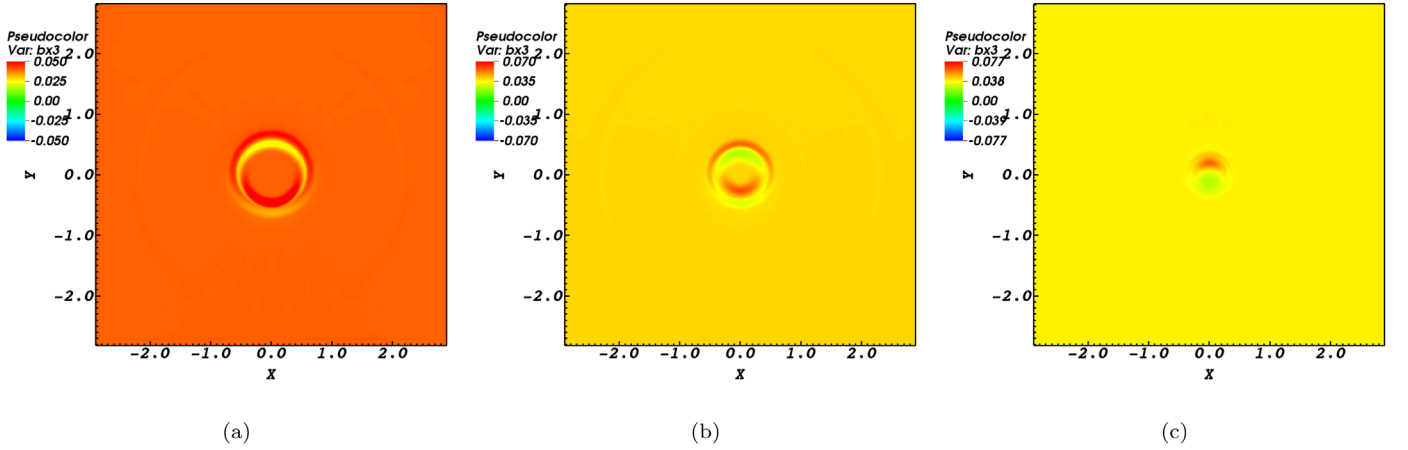


**Figure 7.** The evolution of  $b_z$  (z component of magnetic field) at the fan plane for  $t = 0.3$  s,  $t = 0.5$  s,  $t = 0.6$  s, and  $t = 0.8$  s.

For  $\epsilon \geq 1$ , field lines are aligned parallel to the  $y$ -axis, and for  $0 \leq \epsilon \leq 1$  magnetic field lines predominantly run parallel to the  $x$ -axis. If the coefficient  $\epsilon = 1/2$  is considered, the null point will be isotropic. In this study, if we apply  $\epsilon = 1$  then the null point would be nonisotropic.

This magnetic field can be expressed in terms of a vector potential as follows:

$$\mathbf{A}_0 = [zy, -\epsilon xz, (1 - \epsilon)xy]. \quad (6)$$

Specific quantitative amounts of the initial equilibrium setup are applied to be suitable for the solar coronal plasma:  $\rho_0 = 10^{-12} \text{ kg m}^{-3}$  and  $C_s = 0.129 \text{ Mm s}^{-1}$ . While we would like to study the behavior of the current density accumulation and its following plasma flow due to MHD waves propagation around the 3D magnetic null-point, the magnetic-flux-based coordinate system considers that each direction describes a definite MHD wave mode. The  $A_0$  direction corresponds to the Alfvén wave, longitudinal perturbations along  $B_0$  are associated

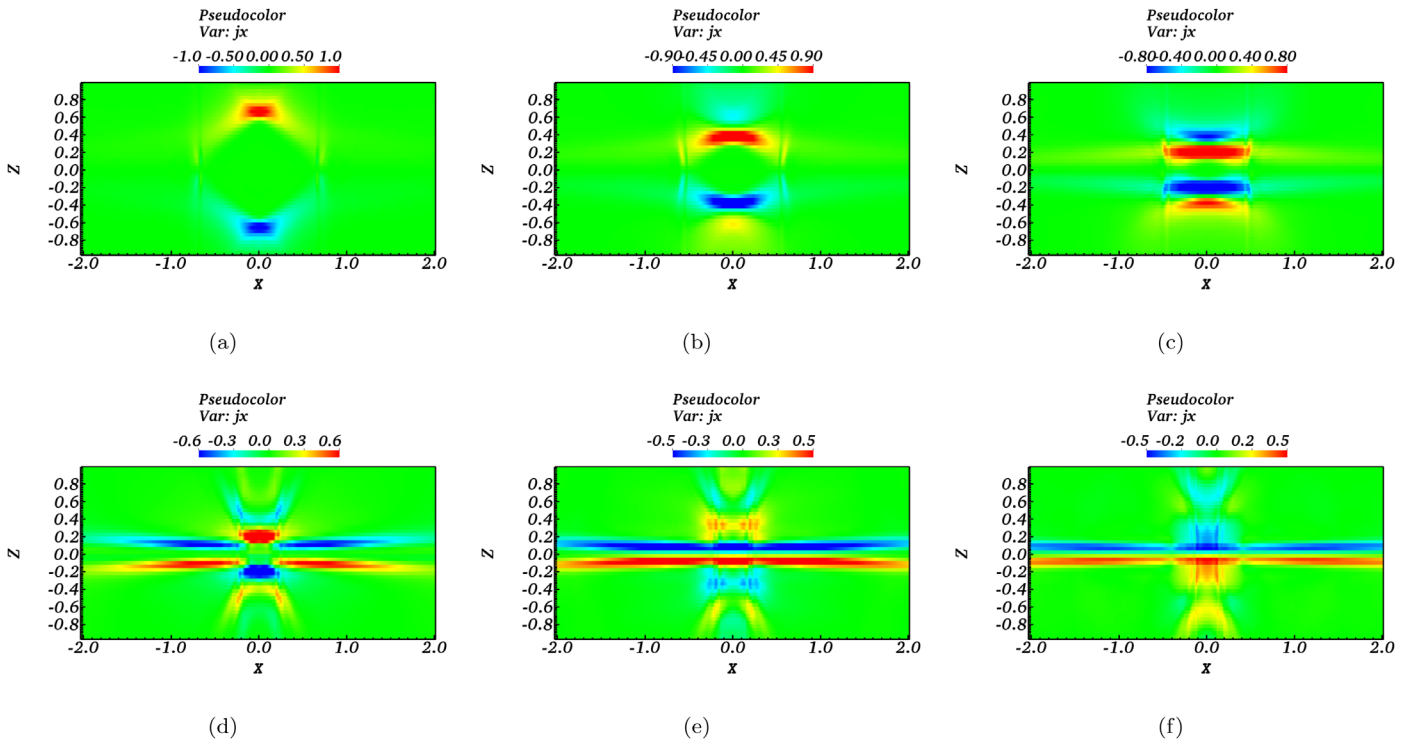


**Figure 8.** Numerical solution of  $j_x$  ( $x$  component of current density) at the  $xz$  plane including the spine axis that is coincident with the  $z$ -axis for  $t = 0.4$  s,  $t = 0.5$  s,  $t = 0.6$  s,  $t = 1.0$  s,  $t = 1.1$  s, and  $t = 1.2$  s.

with the slow mode and the  $C = A_0 \times B_0$  direction is allocated to the fast mode.

### 3. Numerical Results and Discussion

#### 3.1. Initial Alfvén Wave Pulse

First, we consider a single circular Alfvén wave pulse at a definite distance from the magnetic null point. At  $t = 0$  the profile

$$V \cdot A = v_A = A_0 \frac{x}{(x^2 + y^2)} \sin \left[ \pi \frac{\sqrt{x^2 + y^2} - r_1}{r_0} \right] \quad (7)$$

is imposed in the vicinity of a magnetic null point, where we introduced  $V \cdot C = V \cdot B = 0$  and  $A_0$  as the initial amplitude of the circular Alfvén pulse. Note that  $v_A$  defines the wave along the  $A$  direction (Alfvén wave), and not the Alfvén speed, which is denoted by  $C_A$ . It must be noted that there is no preferential alignment of the initial pulse to the magnetic null point and also the spine axis.

High-resolution shock-capturing PLUTO code is used to solve MHD Equations (1)–(4) (Mignone et al. 2007). Typical values of the initial pulse are defined as  $r_0 = 1$  Mm and  $r_1 = 5$  Mm. The background equilibrium plasma has been considered to be static. Besides, the spatial selection for the initial torsional Alfvén pulse is somehow similar to the magnetoacoustic ( $m = 0$ ) mode in the simulation setup of Gruszecki et al. (2011) and Sabri et al. (2020b). Gruszecki et al. (2011) investigated the same pulse shape in the  $x$  and  $y$  directions (i.e., a fast magnetosonic wave pulse) but worked in the zero-beta regime. This simplification enabled them to derive an analytic expression for the radial velocity of the pulse that showed a departure from the azimuthally symmetric  $m = 0$

mode to the  $m = 2$  mode. Besides, they showed that such a pulse with a higher initial amplitude propagates faster. It must be noted that we explored the same initial Alfvén pulse around a 2.5D magnetic null point. It resulted in magnetoacoustic wave perturbations and plasma flow in the vicinity of the magnetic null point without significant current density accumulation and magnetic reconnection (Sabri et al. 2018, 2020b). Since Alfvén waves have a dominant contribution to the coronal heating and genuine coronal magnetic null points are 3D, then Alfvén wave propagation around a 3D magnetic null point is considered for investigation.

#### 3.2. Behavior of Current Densities and Magnetic Field at the Fan Plane

In the majority of astrophysical plasmas with negligible resistivity and viscosity, the generation of small-scale current density becomes so important. In previous 2D and 2.5D studies, because of accumulations of magnetoacoustic waves around the null point that result in small-scale current density excitation, it is asserted that the null point is a possible place for plasma heating.

In both the solar corona and magnetosphere of the Earth, numerous theoretical and also observational studies reported that 3D null points and separators might be areas for the preferential current density generation and plasma heating (Bulanov & Olshansky 1984). Magnetic structure around the magnetic null point is described by the field lines that approach or recede from the null point. These result in two characteristics. The spine is where a single pair of field lines approaches or recedes from the null points in opposite directions. And the fan plane with an infinite number of field lines recedes or approaches from the null point through that surface. It must be noted that the spine axis does not divide topological regions

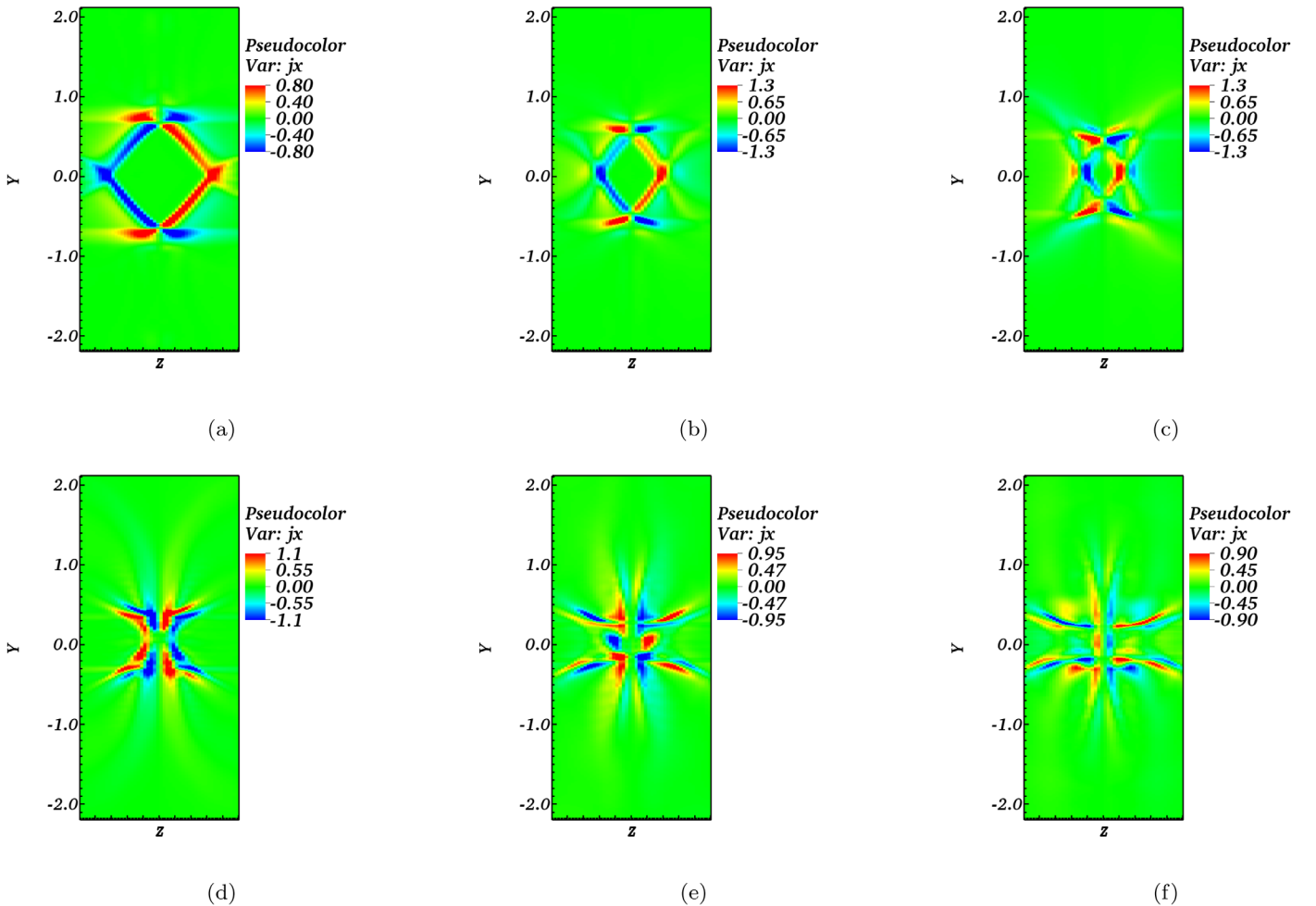


**Figure 9.** Numerical solution of  $j_x$  ( $x$  component of current density) at the  $yz$  plane that includes the spine axis for  $t = 0.4$  s,  $t = 0.5$  s,  $t = 0.6$  s,  $t = 0.8$  s,  $t = 1.0$  s, and  $t = 1.1$  s.

and is just a line, but it has a significant geometrical property. Meanwhile, the fan plane is a separatrix surface that separates unique topological regions. The behavior of current density accumulations in both categories of the 3D structure is investigated here.

Here the current density accumulation profile of the fan plane is illustrated. At first snapshots of the  $x$  component of the current density are shown in Figure 2. At the initial time when the Alfvén wave and its induced magnetoacoustic perturbations do not arrive at the null point, the  $x$  component of the current density is zero as expected. As shown in panels (a) and (b) of Figure 2, circular current density accumulation happens at  $t = 0.3$  s and  $t = 0.5$  s. At the other times it misses its initial circular shape. It is very interesting that it has oscillatory behavior. This means that, as shown in panels (c) and (d), current density accumulates at the null point along the  $x$ -axis. While in panel (e), current density focuses at the null point along the  $y$ -axis. According to panels (c)–(f), the direction of the current density accumulation around the null point changes frequently from  $x$  to  $y$ . This frequent perpendicular behavior of the current density accumulations is called the oscillatory behavior of the  $x$  component of the current density that could refer to the magnetic reconnection.

Brown & Priest (2001) expressed that determining magnetic reconnection locations in complex 3D structure is an important problem. They reported that perhaps magnetic reconnection

happens where strong current densities generate. But in this study, it is shown that oscillatory magnetic reconnection takes place at the fan plane for the  $x$  component of current density while the strong current density focuses along the spine axis, according to Figure 4. It could be concluded that the magnetic reconnection process does not depend on the magnitude of the current density in 3D structure. Perhaps it happens because the fan plane encompasses separate unique topological regions, while the spine axis does not have this characteristic and is just a line without separate topological regions.

Furthermore, the  $y$  component of the current density profile is shown in Figure 3. Note the  $y$  component of the current density also has a circular shape and concentrates at the null point without any significant variation of its initial shape according to Figures 3(a)–(f). It is interesting that while the  $x$  and  $y$  components of the current density have almost the same amplitudes, just the  $x$  component of the current density shows oscillatory behavior.

Finally, the  $z$  component of the current density is also illustrated in Figure 4. The  $z$  component of the current density has a circular shape like the initial Alfvén pulse and it accumulates at the null point, according to panels (a)–(c) of Figure 4. Then it could lead to the heating at the null point even at the 3D magnetic structure. The amplitude of the  $z$  component of the current density, the current parallel to the spine, outweighs around 10 times the other components of current

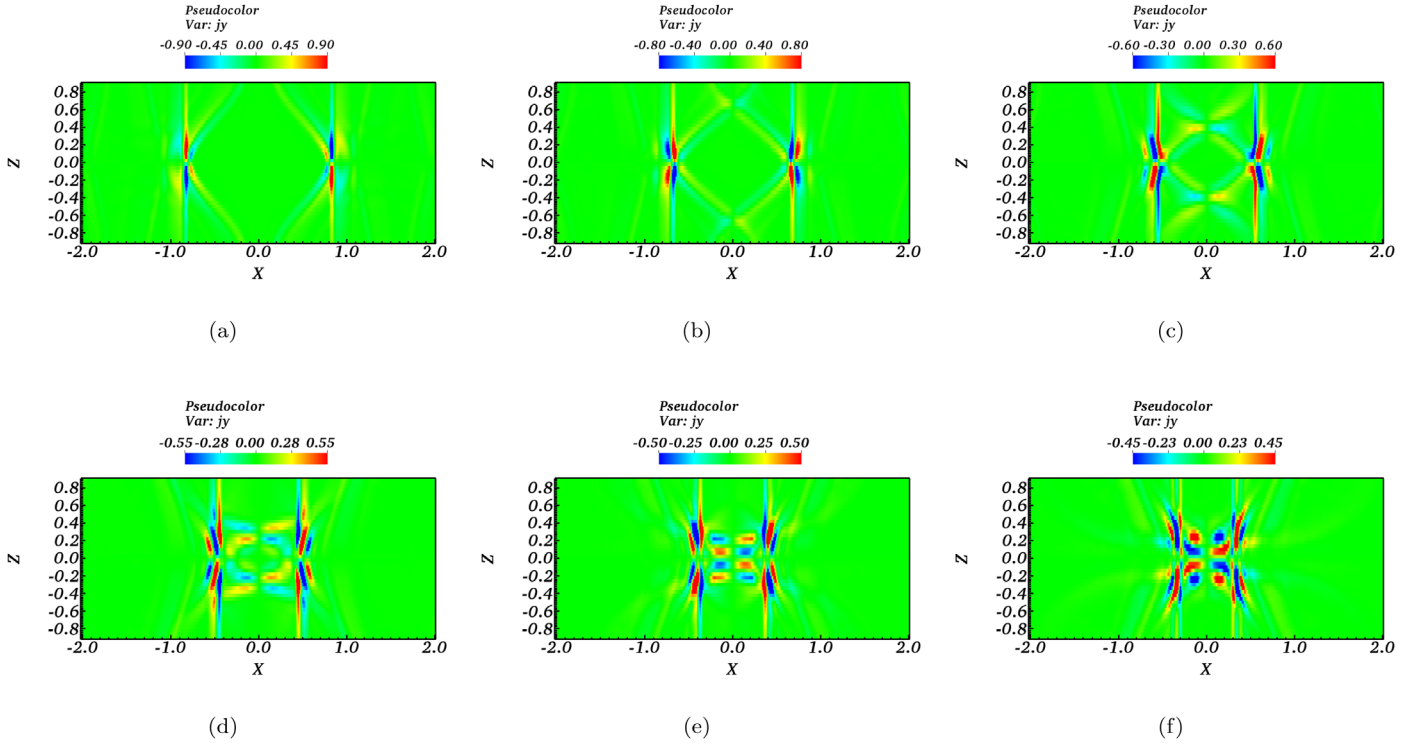


**Figure 10.** Numerical solution of  $j_y$  (y component of current density) at the  $xz$  plane including the spine axis for  $t = 0.3$  s,  $t = 0.4$  s,  $t = 0.5$  s,  $t = 0.6$  s,  $t = 0.7$  s, and  $t = 0.8$  s.

densities as would be expected for an Alfvén wave. Interestingly this significant current density accumulation for the  $z$  component does not show the oscillatory behavior and then magnetic reconnection. Meanwhile, the  $x$  component of the current density with a small amplitude shows the oscillatory behavior.

Above all, it is found that propagation of the Alfvén wave around the 3D magnetic null point leads to current density excitations at the fan plane. The important point is that at the fan plane, all three components of the current density focus around the null point. Therefore, the magnetic null point could be a place that plasma heating and magnetic reconnection happen. Fletcher et al. (2001) observationally showed that magnetic reconnection at a 3D null point might be responsible for some solar flares. Then it is realized that 3D null points have a high possibility of magnetic reconnection. Therefore, more studies are needed to show the behavior of the current density and plasma flow around the 3D magnetic null point. One of the aims of this research is also to provide some pictures of plasma flow to define their behavior around the 3D magnetic null point.

Pontin & Galsgaard (2007) reported that, due to strong magnetic field perturbations in comparison with the background field, nonlinear coupling may occur. They asserted that the nonlinear Alfvén wave may also couple to the magnetoacoustic modes that are attracted to the null point. Because of that, snapshots of the magnetic fields are provided in Figure 5, 6, and 7. It is evident that there are magnetic field perturbations in each of the three directions. It is very interesting that this behavior of magnetic field perturbations does not appear in our previous work where we studied the behavior of the same initial Alfvén wave propagation around the 2.5D magnetic null point (Sabri et al. 2020a). In that study, the magnetic field did not experience any perturbations during the simulation time.

Note that every parameter and situation in this research and our previous work (Sabri et al. 2020a) are the same. Then, it could be expressed that magnetic field perturbations and their following effect on the propagation of the Alfvén wave in the vicinity of the null point are related to the nonlinear coupling that occurs dominantly in complex 3D structure.

### 3.3. Behavior of Current Densities along the Spine Axis

To understand how current density accumulates at planes that involve a spine axis, snapshots of the current densities at the  $yz$  and  $xz$  planes are depicted. It must be noted that  $z$  is a spine axis. In fact, one of the separatrices of the 2D X-point is missed in transition to the 3D structure. As a matter of fact, a 3D structure includes a single separatrix plus spine axis. Note that one of the separatrix surfaces converts to the spine axis.

The  $x$  component of the current density profile at the  $xz$  plane is shown in Figure 8. To illustrate the exact current density accumulation alignment, zoomed snapshots are considered. Panel (a) of Figure 8 illustrates the current density profile at  $t = 0.4$  s. It shows that at the initial time of the simulation, current density has an almost circular shape. So, except for the fan plane, the current density could focus around the null point even at planes with a spine axis. But other snapshots that define the current density profile during the simulation time illustrate current density focusing along the spine axis and around the null point. Panels (d)–(f), which dominantly show that the current density accumulations align the spine axis, interestingly involve phase behavior for the current density alignment along the spine axis in comparison with ones around the null point. Comparing Figures 2 and 8 illustrates the high-amplitude of the current density at the  $xz$  plane that includes the spine axis. The fact is that it was expected because of the initial Alfvén pulse. Nevertheless, it is very interesting that it does not show the

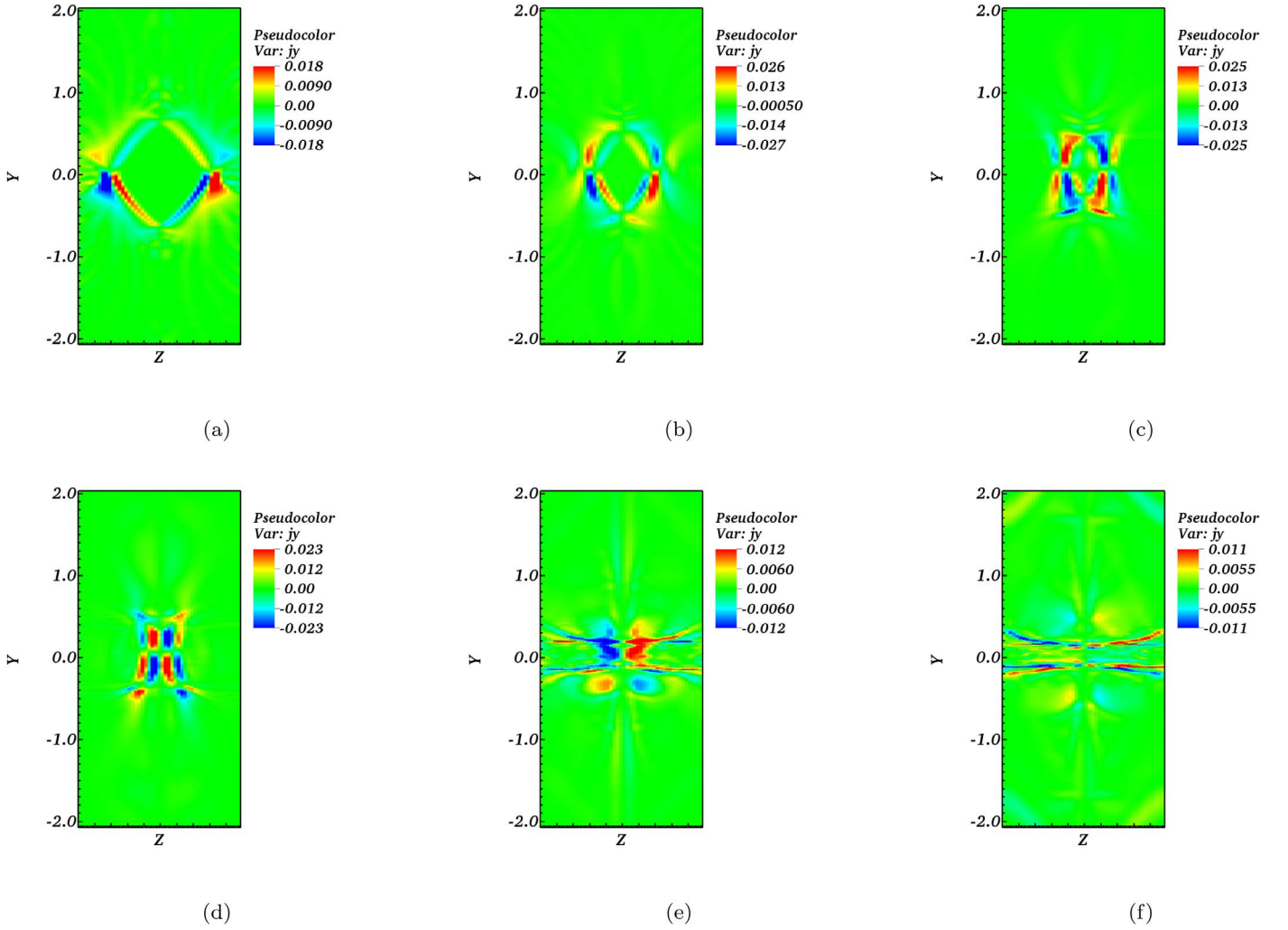


**Figure 11.** Numerical solution of  $j_y$  ( $y$  component of current density) at the  $yz$  plane including the spine axis that is coincident with the  $z$ -axis for  $t = 0.4$  s,  $t = 0.5$  s,  $t = 0.6$  s,  $t = 0.7$  s,  $t = 1.2$  s, and  $t = 1.3$  s.

oscillatory behavior and magnetic reconnection at the  $xz$  plane while it has a high amplitude at this plane in comparison with the fan plane.

Since magnetic reconnection happens just for the  $x$  component of the current density at the fan plane, the unsymmetrical behavior of the  $x$  and  $y$  components of the current density is shown. Here, we have a profile of the  $x$  component of the current density at the  $yz$  plane that again includes the spine axis (Figure 9). As is evident in Figures 2, 8, and 9, the current density amplitude at the  $xz$  and  $yz$  planes are almost the same, and they are higher than the current density strength at the fan plane. However, regarding the high current density amplitude at the  $xz$  and  $yz$  planes, none of them shows the oscillatory behavior despite whatever happens at the fan plane with a small current density. Therefore, against a bit of the same current density amplitude at the  $xz$  and  $yz$  planes, none of them shows the oscillatory behavior. Interestingly, as is evident in panels (a)–(d) of Figure 9, current density accumulates around the null point at the  $yz$  plane without any significant focusing along the spine. Meanwhile, there is also current density accumulation along the spine axis at  $t = 1.0$  s and  $t = 1.1$  s (panels (e) and (f) of Figure 9). So the current density accumulates around the null point and also along the spine axis.

The  $y$  component of current density variations at the  $xz$  plane is depicted in Figure 10. According to panels (a)–(f) of Figure 10, current density accumulation happens toward the spine axis and also around the null point. The  $y$  component of the current density profile at the  $yz$  plane is also observable in Figure 11. It is clear in panels (a) and (b) of Figure 11, current density focuses around the null point with insignificant amplitude and without any accumulations along the spine. Meanwhile, through the last time, according to panels (e) and (f) of Figure 11, current density also accumulates along the spine axis.

Finally, the spatial variations of the  $z$  component of the current density are plotted at the  $xz$  and  $yz$  planes in Figures 12 and 13. At first glance at Figure 12, it is clear that these snapshots have the dominant current density strengths as expected because of the initial Alfvén pulse that was introduced to the system. In other words, the  $z$  component of the current density contains the main current of the system.

Furthermore, according to panels (a)–(f) of Figure 12, the current density completely accumulates along the spine axis without any refraction around the null point. Even though the magnetic field structure is hyperbolic, the current density accumulates quite uniformly in  $z$ , as would be expected for an Alfvén wave. Furthermore, a profile of the  $z$  component of the

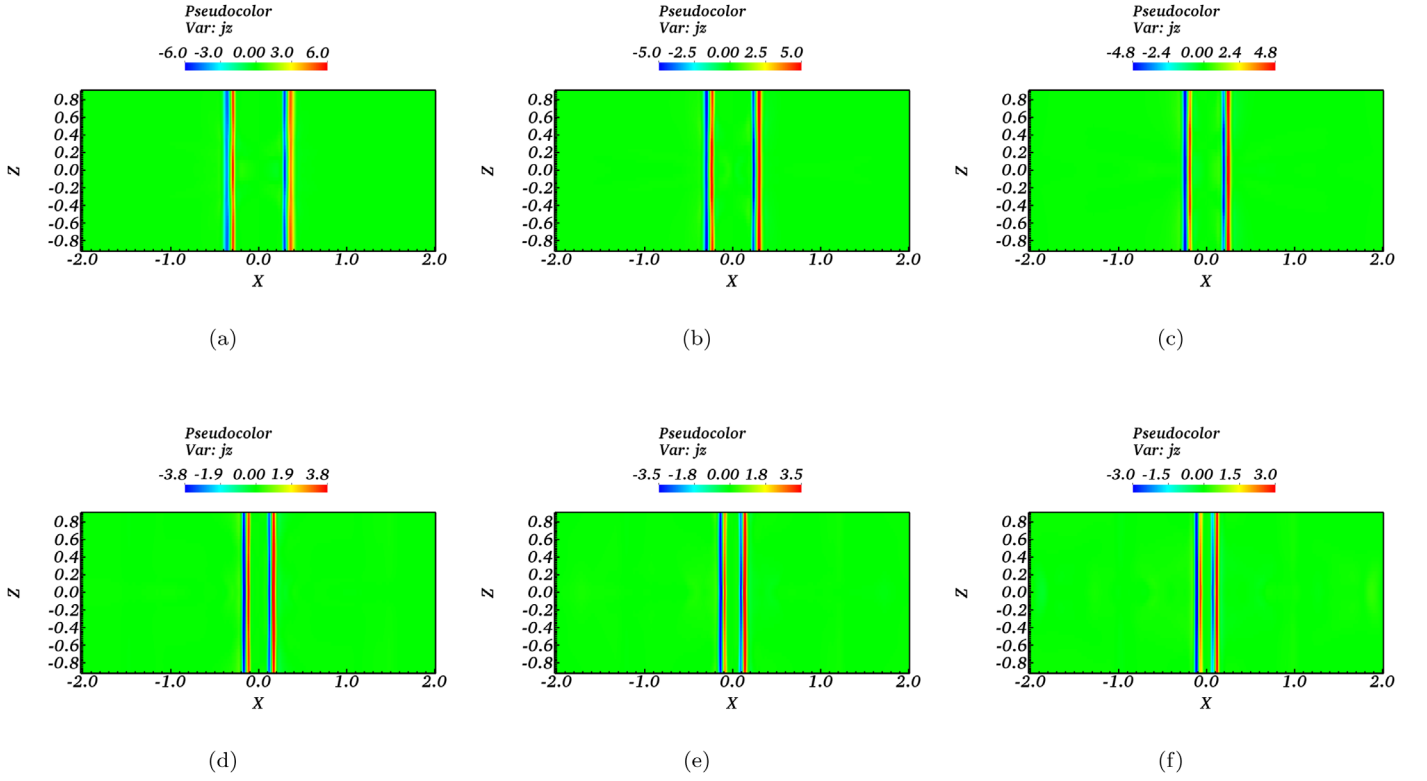


**Figure 12.** Numerical solution of  $j_z$  ( $z$  component of current density) at the  $xz$  plane including the spine axis along the  $z$ -axis. It shows current density excitation along the spine for  $t = 0.8$  s,  $t = 0.9$  s,  $t = 1.0$  s,  $t = 1.2$  s,  $t = 1.3$  s, and  $t = 1.4$  s.

current density at the  $yz$  plane is illustrated in Figure 13. As is clear from panels (a)–(d) of Figure 13, the  $z$  component of the current density also focuses around the null point while there is current density accumulation along the spine axis. Finally, according to panels (e) and (f) of Figure 13, current density accumulates along the spine axis without any refraction through the null point.

It is found that current density accumulations at the fan plane happen around the null point, but in other planes, including the spine axis, current density accumulations take place along the spine and also around the null point. Then it does indeed show that in the 3D magnetic null point, separators, the magnetic null point, and the spine axis are possible places for plasma heating. Longcope (2005) reported that separators are regions for heating of the corona. In this research, it is found that the initial Alfvén wave disturbance that moves along the 3D null point results in current accumulation at the null point, separators, and along the spine. It is also foreseen that those different current orientations in the vicinity of the magnetic null point could result in very different behavior (Pontin et al. 2004, 2005). Moreover, it is apparent that every three components of the current profiles are symmetric at the null. It means that the current density makes a singular spike that is centered on the null point.

### 3.4. Excited Plasma Flow

Fletcher et al. (2001) observationally found that magnetic reconnection at a 3D null point may launch some solar flares. Plasma flow generated by perturbations could help to recognize what kind of magnetic reconnection takes place during the current density variations. Besides the current density behavior, we also investigate the plasma flow generation due to the

current density. It must be noted that the plasma is initially at rest and therefore there is no flow through the boundaries.

Snapshots of the plasma flow are shown in Figures 14–19. If we look back, we would find that Figures 14–16 are similar to the spatial variations of the  $y$  component of the current density. This similarity has encouraged us to consider it analytically.

Along this line, it is expected that the motion equation (Equation (1)) would verify the relation between velocity and current density perturbations. Then, this equation is analyzed in detail considering our system approximation that includes the initial Alfvén pulse. Since Alfvén waves are incompressible, then their propagations do not result in significant perturbations of the plasma density. Therefore, we can rewrite Equation (1) as Equation (5):

$$\rho \left[ \frac{\partial \mathbf{V}}{\partial t} \right] \simeq \left( \frac{1}{\mu} \mathbf{J} \times \mathbf{B} \right). \quad (8)$$

So the following equations are for the  $x$  and  $y$  components of the current density:

$$\rho \left[ \frac{\partial V_x}{\partial t} \right] \simeq \frac{1}{\mu} (j_y b_z - j_z b_y), \quad (9)$$

$$\rho \left[ \frac{\partial V_y}{\partial t} \right] \simeq \frac{1}{\mu} (j_z b_x - j_x b_z). \quad (10)$$

Because of our initial assumptions, the spine axis locates along the  $z$ -axis and the fan plane locates at the  $xy$  plane. Note that the initial Alfvén pulse is introduced at a specific distance from the null point almost along the  $z$ -axis and it propagates toward the fan plane. Since the Alfvén wave is a transverse wave then its propagation basically is accompanied by disturbances of the  $z$

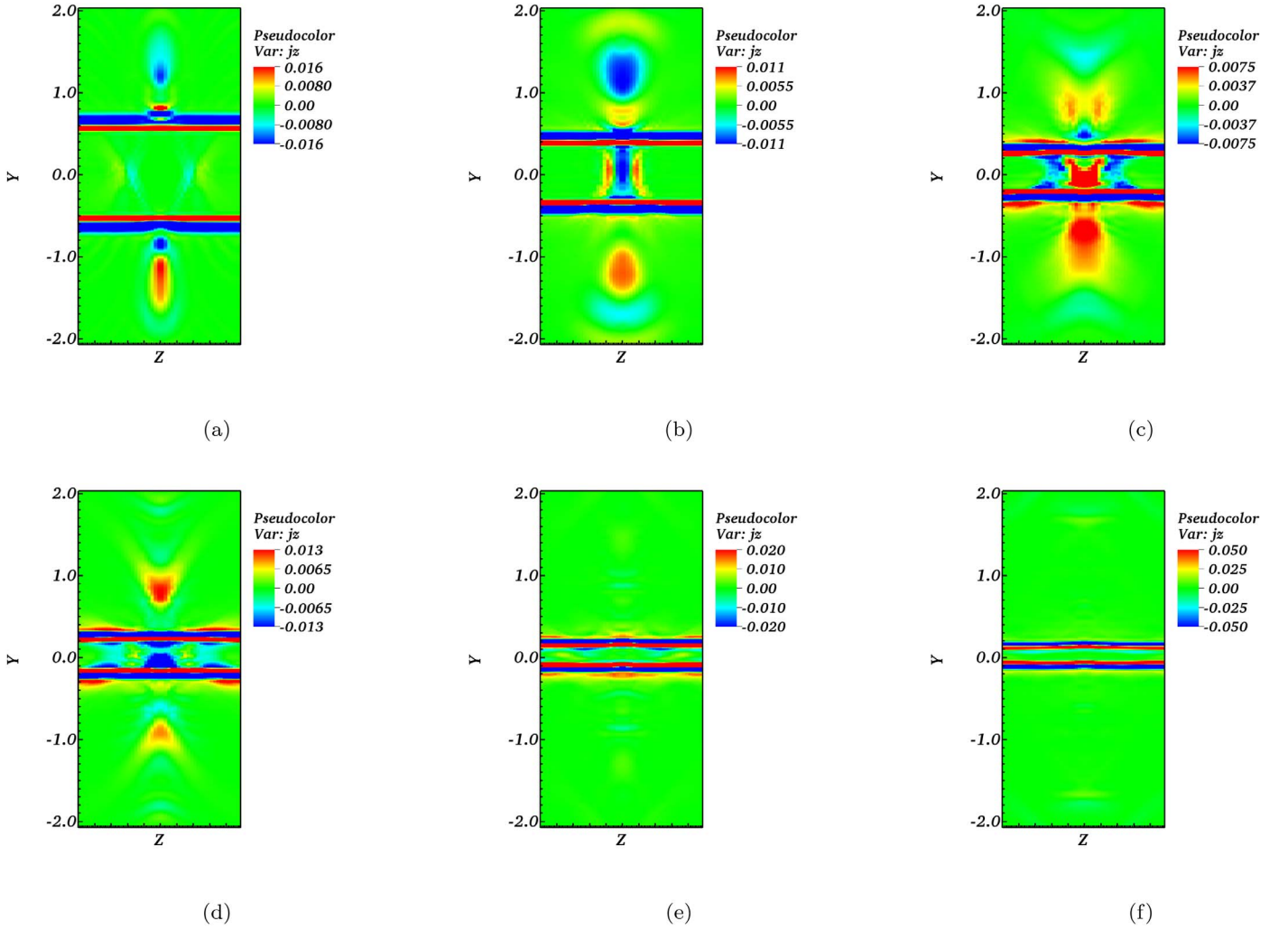


**Figure 13.** Numerical solution of  $j_z$  ( $z$  component of current density) at the  $yz$  plane including the spine axis that is coincident with the  $z$ -axis. It illustrates current density excitation along the spine for  $t = 0.5$  s,  $t = 0.7$  s,  $t = 0.9$  s,  $t = 1.0$  s,  $t = 1.2$  s, and  $t = 1.3$  s.

component of the magnetic field. In other words, perturbation of the  $x$  and  $y$  components of the magnetic field could be negligible in comparison with the  $z$  component. Because of that we neglect  $b_x$  and  $b_y$  in comparison with  $b_z$ . Because of negligible perturbations of the  $x$  and  $y$  components of the magnetic field in comparison with the  $z$  component, that is expected due to the initial Alfvén pulse. So we have the following equations for velocities or plasma flow:

$$\rho \left[ \frac{\partial V_x}{\partial t} \right] \propto j_y, \quad (11)$$

$$\rho \left[ \frac{\partial V_y}{\partial t} \right] \propto -j_x. \quad (12)$$

Then it is analytically shown that the  $x$  component of the plasma flow is proportional to the  $y$  component of the current density and the  $y$  component of the plasma flow profile is treated like the  $x$  component of the current density. It is interesting that our numerical results for plasma flow and current density are consistent with analytical results.

However, more insight may be obtained by investigating the time evolution of current densities and plasma flow according

to Figure 20. Panel (a) of Figure 20 demonstrates the time evolution of the  $x$  component of the plasma flow and the  $y$  component of the current density. It is clear that this plot has almost the same behavior in our numerical results, which is in agreement with Equation (11). Besides, panel (b) of Figure 20 illustrates the time evolution of the  $y$  component of the plasma flow and the  $x$  component of the current density. It is evident that this plot has almost the same inverse behavior in our numerical results, which is in agreement with Equation (12). It means that Alfvén wave propagation in the vicinity of a 3D magnetic null point results in plasma flow that the  $y$  component of the current density defines the  $x$  component of the plasma flow behavior and the  $x$  component of the current density inversely distinguishes behavior of the  $y$  component of the plasma flow. It must be noted that Figure 2 illustrates there is oscillatory current density accumulation, while it did not happen for the  $y$  component of the current density (Figure 3). It is very interesting that comparison between panels (a) and (b) of Figure 20 shows that the  $y$  component of the current density is around 100 times weaker than the  $x$  component of the current density. Then it verifies the oscillatory behavior of the  $x$  component of the current density and also magnetic reconnection.

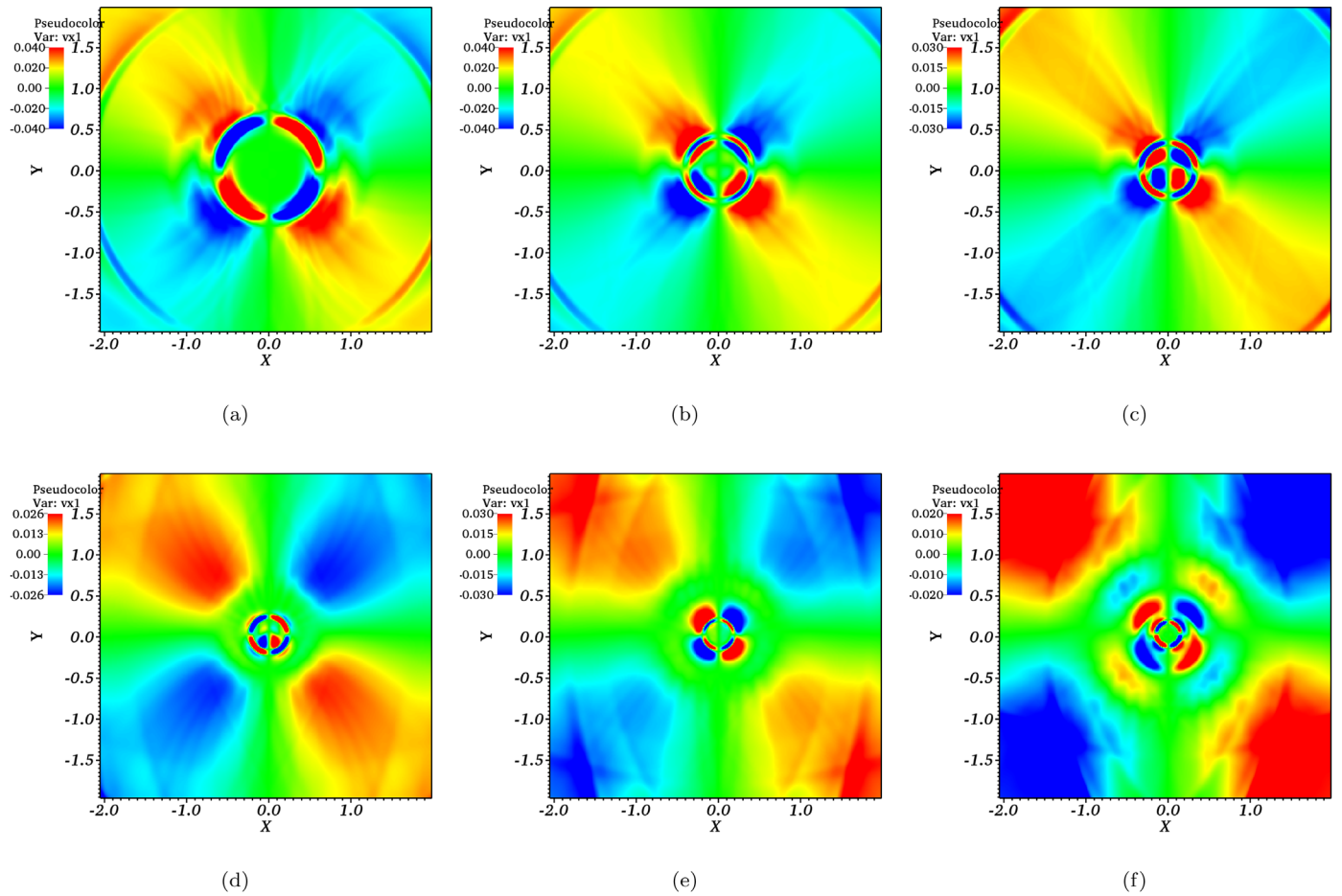


**Figure 14.** Numerical solution of  $v_x$  ( $x$  component of magnetic field) at the  $xy$  plane for  $t = 0.5$  s,  $t = 0.7$  s,  $t = 0.8$  s,  $t = 1.0$  s,  $t = 1.1$  s, and  $t = 1.2$  s.

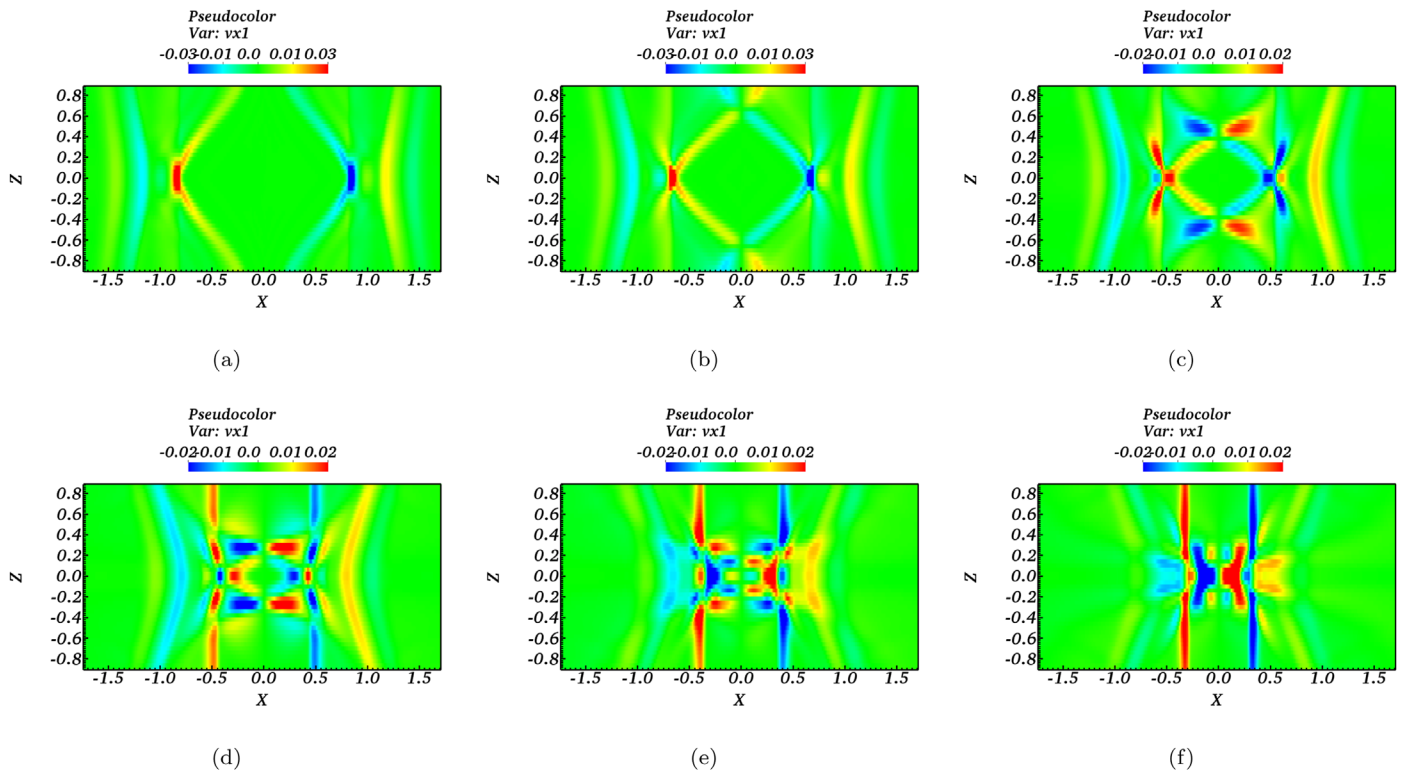


**Figure 15.** Numerical solution of  $v_x$  ( $x$  component of magnetic field) at the  $xz$  plane for  $t = 0.3$  s,  $t = 0.4$  s,  $t = 0.5$  s,  $t = 0.6$  s,  $t = 0.7$  s, and  $t = 0.8$  s.

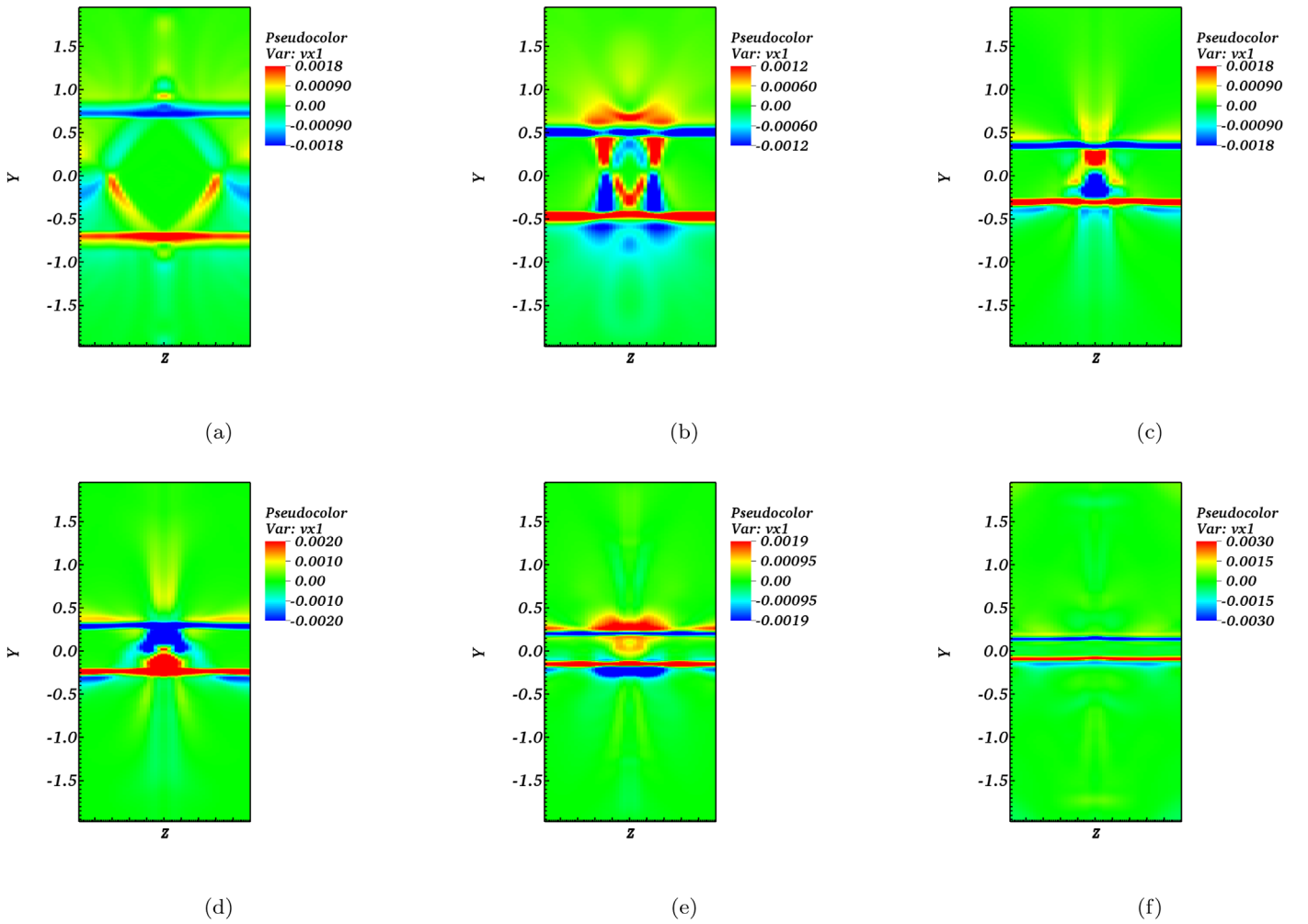


**Figure 16.** Numerical solution of  $v_x$  ( $x$  component of magnetic field) at the  $yz$  plane for  $t = 0.4$  s,  $t = 0.6$  s,  $t = 0.8$  s,  $t = 0.9$  s,  $t = 1.1$  s, and  $t = 1.3$  s.

#### 4. Conclusions

Magnetic null points and MHD waves are both prevalent in many astrophysical plasmas, including the solar atmosphere. Here we investigate the propagation of the Alfvén wave around the 3D proper magnetic null point by numerically solving the resistive, finite plasma beta MHD equations using the PLUTO code. In astrophysical plasmas, such as the solar corona, 3D magnetic null points are very complicated. In such points, specifying areas where dynamic phenomena and energy release may happen is a key and nontrivial problem. In ideal MHD evolution, such events occur only at locations where high current densities may be created. Then, current density excitations are a key characteristic. Hence, the nature of current densities at the 3D structure is explored here.

In this paper, the null-point structure, preconditions, equilibrium variables, and assumptions are studied under solar coronal conditions. We pursue the nonlinear evolution of an initially force-free three-dimensional magnetic null point subject to an initial Alfvén pulse. The results illustrate how magnetic field components are dynamically evolved, how current density accumulations formed in the vicinity of the magnetic null point, and also how current density accumulations accompany the plasma flow.

It is very interesting that in the case of the 2.5D structure that we studied before (Sabri et al. 2018), the  $x$  and  $y$  components of

the magnetic field did not include any perturbations. In this work, the same initial Alfvén pulse was introduced, and the effect of the 3D magnetic topology on current density profiles and plasma flow was explored. It is found that magnetic field perturbations and their following effect on the propagation of the Alfvén wave in the vicinity of the null point are related to the nonlinear coupling that are dominant in complex 3D structure in comparison with the 2.5D structure.

It is expected that disturbances that are essentially Alfvénic propagate along the background magnetic field lines. Therefore, current density accumulation happens toward the spine axis. Therefore, it is expected that the preferential amount of the current density accumulates along the spine axis ( $z$  direction). But it is found Alfvén wave propagation toward the null point leads to the current density accumulation toward the spine axis or separator and also around the null point.

In summary, the following main results are found:

1. It is found that the oscillatory magnetic reconnection takes place at the fan plane for the  $x$  component of the current density, while the strong current density is focused along the spine axis. It could be concluded that the magnetic reconnection process does not depend on the strength of the current density in the 3D structure. Maybe it happens because the fan plane encompasses separate unique topological regions, while the spine axis

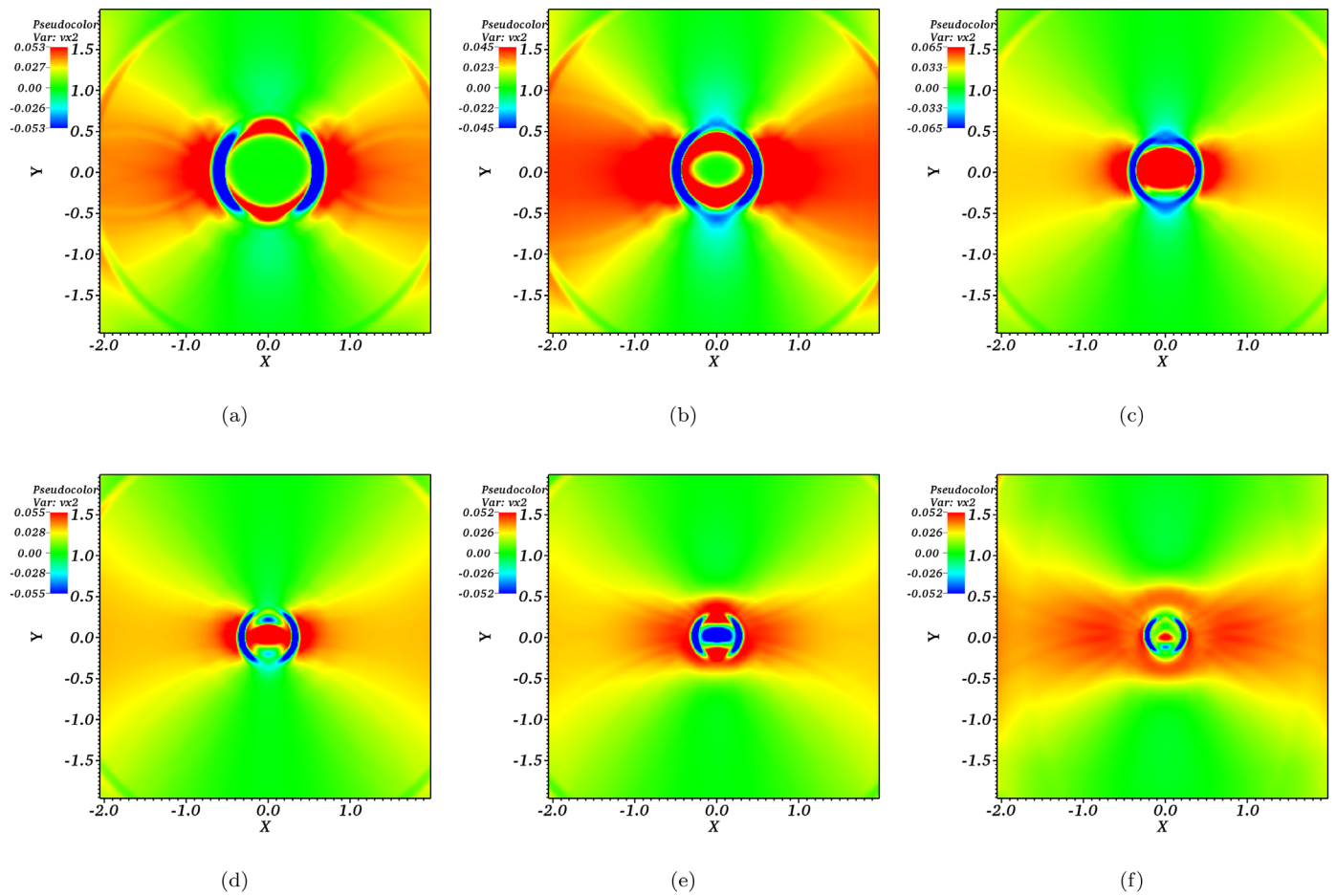


**Figure 17.** Numerical solution of  $v_x$  ( $x$  component of magnetic field) at the fan plane for  $t = 0.5$  s,  $t = 0.6$  s,  $t = 0.7$  s,  $t = 0.8$  s,  $t = 0.9$  s, and  $t = 1.0$  s.

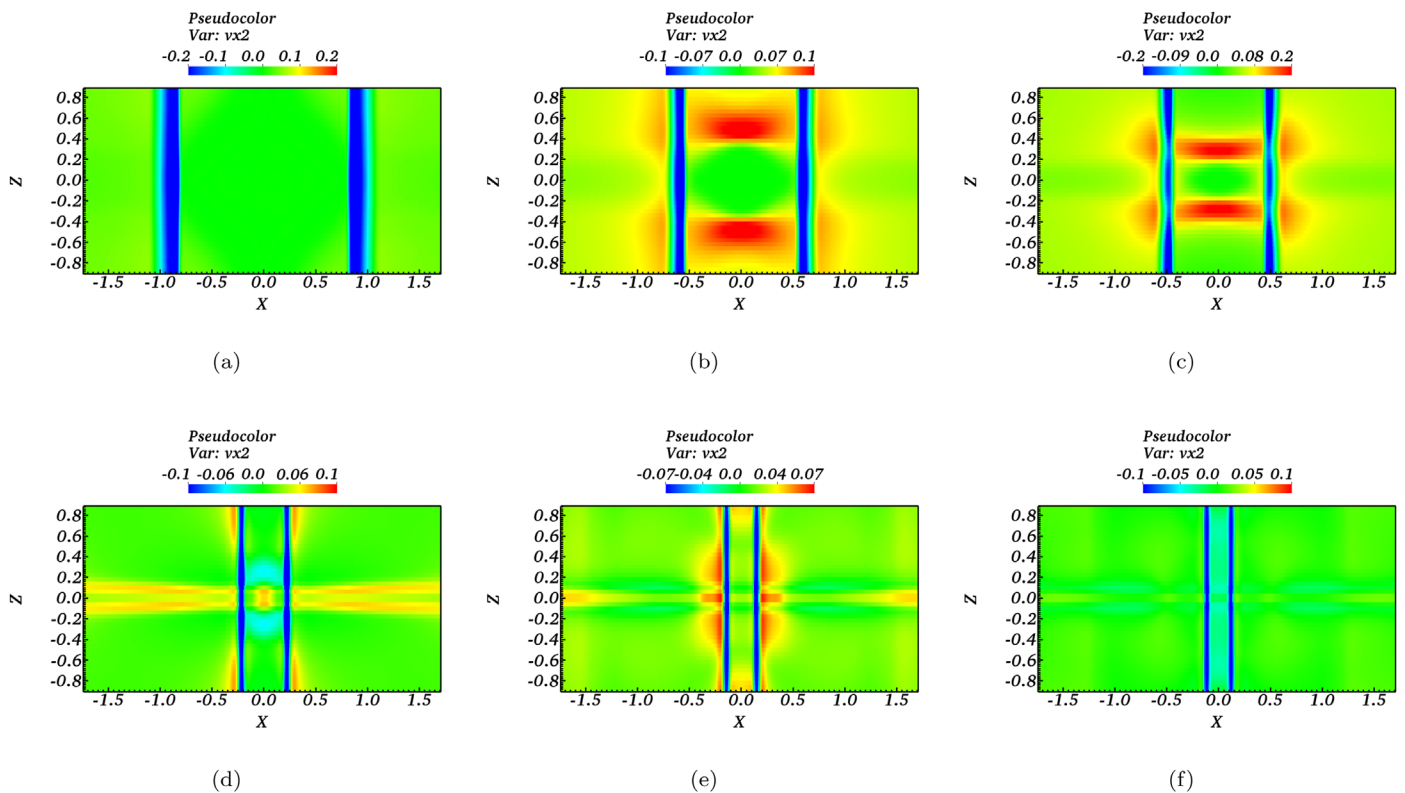


**Figure 18.** Numerical solution of  $v_x$  ( $x$  component of magnetic field) at the  $xz$  plane for  $t = 0.3$  s,  $t = 0.5$  s,  $t = 0.6$  s,  $t = 1.0$  s,  $t = 1.2$  s, and  $t = 1.3$  s.

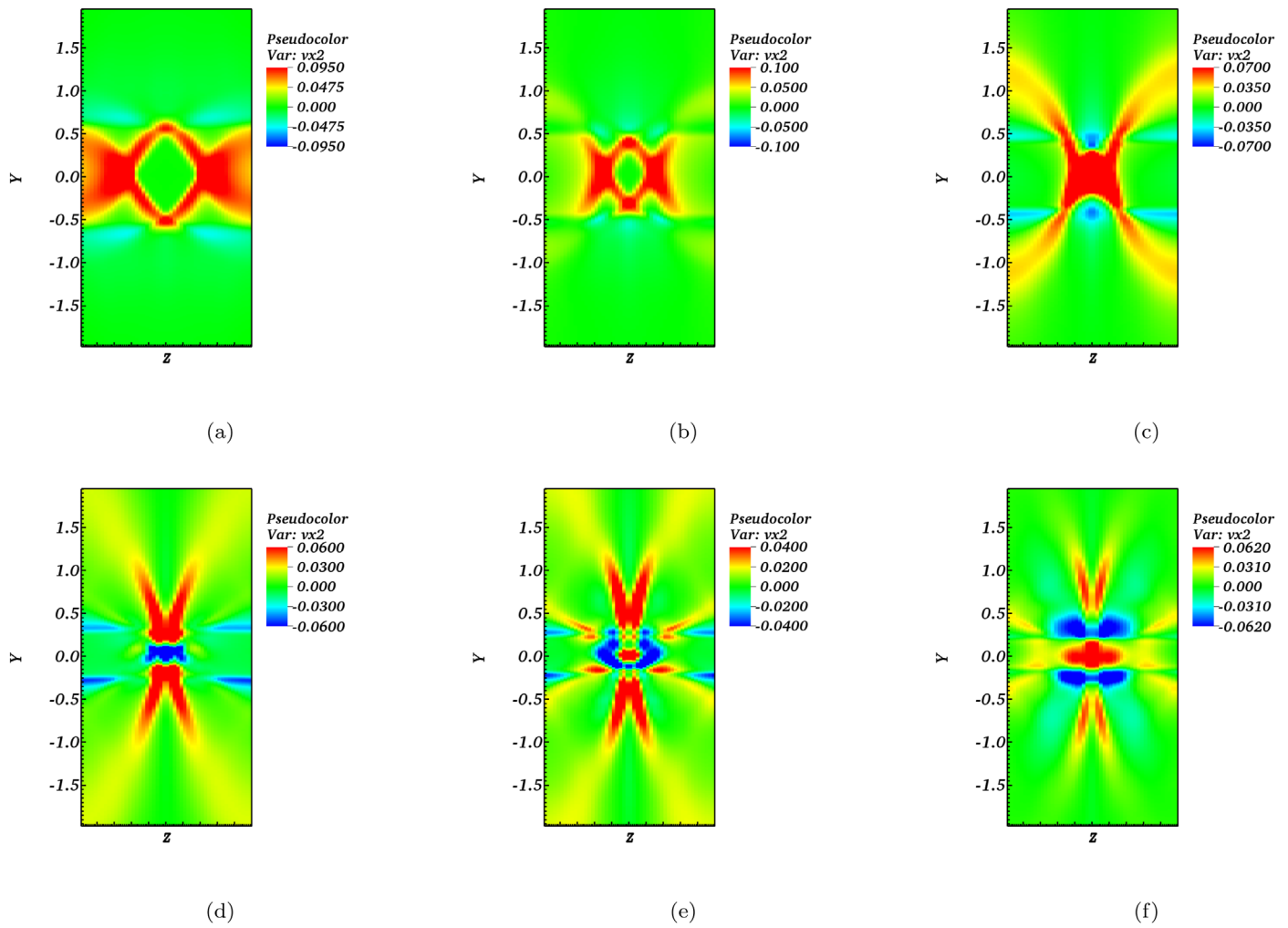


**Figure 19.** Numerical solution of  $v_x$  ( $x$  component of magnetic field) at the  $yz$  plane for  $t = 0.5$  s,  $t = 0.6$  s,  $t = 0.7$  s,  $t = 0.9$  s,  $t = 1.0$  s, and  $t = 1.1$  s.

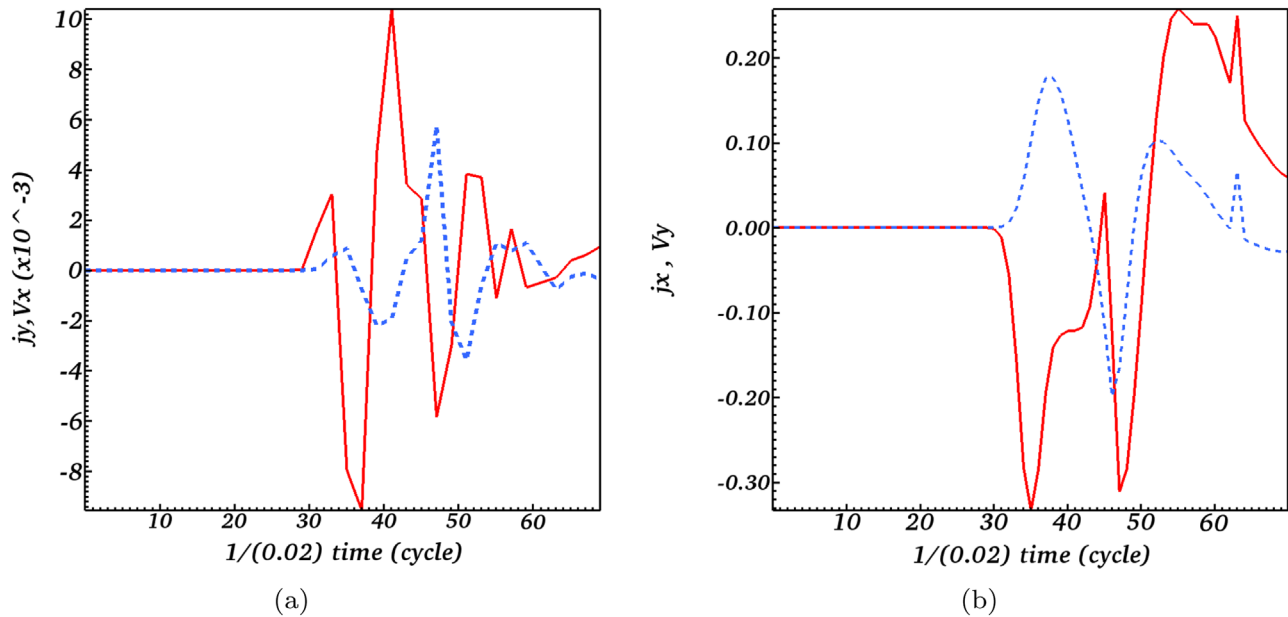


**Figure 20.** (a) Time variation of the  $x$  component of the current density (red solid line) and the  $y$  component of the plasma flow (blue dashed line) at the null point  $(0, 0, 0)$ , (b) time variation of the  $y$  component of the current density (red solid line) and the  $x$  component of plasma flow (blue dashed line) at the null point  $(0, 0, 0)$ .

does not have this characteristic and is just a line without separate topological regions.

2. It is found that current density accumulations at the fan plane happen around the null point without any alignments through the axis. However, in other planes including the spine axis, current density accumulations take place along the spine and also around the null point. Then it does indeed show that in the 3D magnetic null point, separators, the spine axis, and also the null point itself are possible places for the plasma heating.
3. It is apparent that each of the three components of the current profiles are symmetric at the null point. It means that the current density makes a singular spike that is centered on the null point.
4. Our results also imply that Alfvén wave propagation in the vicinity of a 3D magnetic null point results in plasma flow where the  $y$  component of the current density mostly defines the  $x$  component of the plasma flow behavior and the  $x$  component of the current density inversely distinguishes the behavior of the  $y$  component of the plasma flow.

The authors would like to thank the referee for valuable and helpful comments and suggestions that helped improve this work significantly. This research is financially supported by a research grant of the University of Tabriz (S/2762). For the computations we used the infrastructure of the VSC Flemish Supercomputer Center, funded by the Hercules foundation and the Flemish Government—department EWI.

#### ORCID iDs

S. Sabri  <https://orcid.org/0000-0002-7947-7797>  
 H. Ebadi  <https://orcid.org/0000-0002-3914-6141>  
 S. Poedts  <https://orcid.org/0000-0002-1743-0651>

#### References

- Brown, D. S., & Priest, E. R. 2001, *A&A*, 367, 339  
 Bulanov, S. V., & Olshanetsky, M. A. 1984, *PhLA*, 100, 35  
 Close, R. M., Parnell, C. E., & Priest, E. R. 2004, *SoPh*, 225, 21  
 Copil, P., Voitenko, Y., & Goossens, M. 2008, *A&A*, 478, 921  
 Craig, I. J. D., & McClymont, A. N. M. 1993, *ApJ*, 405, 207  
 Craig, I. J. D., & Pontin, D. I. 2014, *ApJ*, 788, 177  
 Filippov, B. 1999, *SoPh*, 185, 297  
 Fletcher, L., Metcalf, T. R., Alexander, D., Brown, D. S., & Ryder, L. A. 2001, *ApJ*, 554, 451  
 Freed, M. S., Longcope, D. W., & McKenzie, D. E. 2015, *SoPh*, 290, 467  
 Galsgaard, K., & Nordlund, A. 1996, *JGR*, 102, 231  
 Galsgaard, K., & Pontin, D. I. 2011a, *A&A*, 534, A2  
 Galsgaard, K., & Pontin, D. I. 2011b, *A&A*, 529, A20  
 Galsgaard, K., Priest, E. R., & Titov, V. S. 2003, *JGRA*, 108, 1042  
 Gruszecki, M., Vasheghani Farahani, S., Nakariakov, V. M., & Arber, T. D. 2011, *A&A*, 531, A63  
 Guo, J. N., Buchner, J., Otto, A., et al. 2010, *A&A*, 513, A73  
 Hollweg, J. V. 1971, *JGR*, 76, 5155  
 Longcope, D. W. 2005, *LRSP*, 2, 293  
 Longcope, D. W., Brown, D. S., & Priest, E. R. 2003, *PhPI*, 3, 2885  
 McLaughlin, J. A., Ferguson, J. S. L., & Hood, A. W. 2008, *SoPh*, 251, 563  
 Mignone, A., Bodo, G., Massaglia, S., et al. 2007, *ApJS*, 170, 228  
 Pariat, E., Antiochos, S. K., & DeVore, C. R. 2009, *ApJ*, 691, 61  
 Parker, E. N. 1957, *JGR*, 62, 509  
 Pontin, D. I. 2011, *AdSpR*, 47, 1508  
 Pontin, D. I., Bhattacharjee, A., & Galsgaard, K. 2007, *PhPI*, 14, 052106  
 Pontin, D. I., & Craig, I. J. D. 2005, *PhPI*, 12, 072112  
 Pontin, D. I., & Galsgaard, K. 2007, *JGRA*, 112, A03103  
 Pontin, D. I., Hornig, G., & Priest, E. R. 2004, *GApFD*, 98, 407  
 Pontin, D. I., Hornig, G., & Priest, E. R. 2005, *GApFD*, 99, 77  
 Pontin, D. I., Priest, E. R., & Galsgaard, K. 2013, *ApJ*, 774, 154  
 Priest, E. R., & Forbes, T. 2000, *Magnetic Reconnection. MHD Theory and Applications* (Cambridge: Cambridge Univ. Press)  
 Priest, E. R., & Titov, V. S. 1996, *RSPTA*, 354, 2951  
 Rickard, G. J., & Titov, V. S. 1996, *ApJ*, 472, 840  
 Ruderman, M. S. 1999, *ApJ*, 521, 851  
 Sabri, S., Ebadi, H., & Poedts, S. 2020, *ApJ*, 902, 11  
 Sabri, S., Poedts, S., & Ebadi, H. 2019, *A&A*, 623, A81  
 Sabri, S., Vasheghani Farahani, S., Ebadi, H., Hosseinpour, M., & Fazel, Z. 2018, *MNRAS*, 479, 4991  
 Sabri, S., Vasheghani Farahani, S., Ebadi, H., & Poedts, S. 2020, *NatSR*, 10, 15603  
 Srivastava, A. K., Shetye, J., Murawski, K., et al. 2017, *NatSR*, 7, 43147  
 Stanier, A., Browning, P., & Dalla, S. 2012, *A&A*, 542, A47  
 Su, Y., Veronig, A. M., Holman, G. D., et al. 2013, *NatPh*, 9, 489  
 Sweet, P. A. 1958, in *IAU Symp. 6, Electromagnetic Phenomena in Cosmic Physics*, ed. B. Lehnert (Cambridge: Cambridge Univ. Press), 123  
 Tikhonchuk, V. T., Rankin, R., Frycz, P., & Samson, J. C. 1995, *PhPI*, 2, 501  
 Xiao, C. J., Wang, X. G., Pu, Z. Y., et al. 2006, *NatPh*, 2, 478  
 Zheng, J., Chen, Y., & Yu, M. 2016, *PhysS*, 91, 015601